Optical and Quantum Electronics (2023) 55:1165
https://doi.org/10.1007/s11082-023-05291-w

Gamma irradiation-induced changes in structural, linear/nonlinear optical, and optoelectrical properties of PVB/$BiVO_4$ nanocomposite for organic electronic devices

M. I. A. Abdel Maksoud[1] · Ramy Amer Fahim[2] · Said M. Kassem[2] · A. S. Awed[3]

Received: 2 July 2023 / Accepted: 10 August 2023 / Published online: 12 October 2023

Abstract
Herein, nanocomposite films based on polyvinyl butyral (PVB) and $BiVO_4$ plates were synthesized through solution casting. The present study aims to investigate the impact of varying doses of gamma irradiation (0, 15, 30, 60, and 90 kGy) on the structural, dispersion, linear/nonlinear optical, and optoelectrical properties of PVB/$BiVO_4$ nanocomposite films. The effects of gamma irradiation on various optical characteristics, such as refractive index (n), extinction coefficient (k), and other related parameters, have been observed. The study of dielectric behavior and the derivation of optoelectrical parameters, including high-frequency dielectric constant (ε_∞), plasma frequency (ω_P), relaxation time (τ), and optical mobility ($\mu_{opt.}$), were conducted using the real and imaginary parts of the dielectric constants ε_r and ε_i. In addition, the linear optical susceptibility ($\chi^{(1)}$), the third-order nonlinear optical susceptibility ($\chi^{(3)}$), and the nonlinear refractive index (n_2) were studied as a function of gamma irradiation doses. Furthermore, the results demonstrate that the average oscillator wavelength (λ_0) values, oscillator strength (S_0), and optical conductivity ($\boldsymbol{\sigma_{opt}}$) vary significantly after gamma radiation treatment. Overall, the strong correlations between the linear/nonlinear optical and optoelectrical parameters of the irradiated PVB/$BiVO_4$ nanocomposite films make them suitable for application in flexible organic electronic devices.

Keywords Gamma irradiation · Linear/nonlinear optical · Optoelectrical · PVB · $BiVO_4$

✉ M. I. A. Abdel Maksoud
muhamadmqsod@gmail.com; muhamadabdelmaksoud@gmail.com

[1] Radiation Physics Department, National Center for Radiation Research and Technology (NCRRT), Egyptian Atomic Energy Authority (EAEA), Cairo, Egypt

[2] Radiation Protection and Dosimetry Department, National Center for Radiation Research and Technology (NCRRT), Egyptian Atomic Energy Authority (EAEA), Cairo, Egypt

[3] Higher Institute for Engineering and Technology at Manzala, Manzala, Egypt

1 Introduction

Polyvinyl butyral (PVB) material has been thoroughly studied and frequently utilized due to its high durability, superior optical clarity, and facile adherence to varied surface characteristics (Ipakchi et al. 2020; Wen et al. 2019; Lei et al. 2019; Azad and Mohsennia 2020). Recently, Lee et al.(Lee et al. 2019), have developed a composite material based on PVB and silver nanowires, which exhibit outstanding flexibility, mechanical strength, and smoothness. The purpose of this composite material is to increase the efficiency with which light can be extracted from flexible organic light-emitting diodes (OLEDs).

Composites based on polymers have been at the cutting edge of materials science research in recent years due to their distinct characteristics. As a result of their ability to modify their optical, electrical, and mechanical properties, they are promising candidates for various applications, including electronic devices, detectors, photovoltaic technology, lasers, and medical devices (Badawi et al. 2019). Since the growth of optical material applications is still in the early stages of development, it is essential to produce new materials with enhanced properties (Beecroft and Ober 1997). Enhancing linear and nonlinear optical parameters (optical band gap, linear and nonlinear refractive index, and third-order nonlinear susceptibility) is the primary objective of evaluating organoelectronic materials (Stepanov 2019; Soliman and Vshivkov 2019; Waszkowska et al. 2020). The nature of transitions between the highest occupied molecular orbital (HOMO) and the lowest unoccupied molecular orbital (LUMO) can be better understood by analyzing the absorption edge and refractive index (Ebnalwaled and Thabet 2016). These parameters can be optimized by modifying the additives' nature, size, and distribution within a polymer matrix (Stepanov 2019). The electrochemical characteristics of composites are influenced by the interactions between their organic and inorganic components. The potential concern of polymer chain diffusion into the host structure depends upon the chains' length and the pores' dimensions. The nanocomposites exhibit promising potential for implementation in optoelectronic applications (Nguyen 2011). Numerous semiconducting materials exhibit promising potential for utilization in optoelectronics applications, including SnO/SnO_2 (Siva et al. 2021; Dhatarwal et al. 2020), ZnO (Choudhary 2018), Al_2O_3–SiO_2(Dhatarwal and Sengwa 2021), $BaTiO_3$(Beena and Jayanna 2019), and $SrTiO_3$(Taha and Alzara 2021). Among semiconductors, bismuth vanadate ($BiVO_4$) is a semiconductor that is n-type, direct, and has a narrow bandgap of 2.4 eV. This characteristic facilitates the absorption of visible light within the solar spectrum, which is important for photovoltaic conversion efficiency (Khan et al. 2017; Batool et al. 2021; Shao et al. 2022).

Upon ionization and excitation of the molecules within the polymer composite, the gamma radiation induces the breaking of the main bonds, cross-linking, chain scission, and the generation of free radicals within the polymer nanocomposite. This current approach for the growth of nanoparticles NPs is effective and eco-friendly, as it does not involve using potentially dangerous substances, in contrast to chemical and physical strategies (Abdel Maksoud et al. 2023, 2022; Alshahrani et al. 2021a, 2021b; El- Mallah et al. 2020).

Herein, for the first time, the solid-state approach was utilized to synthesize $BiVO_4$ nanoparticles, which were then incorporated with polyvinyl butyral (PVB) to develop a PVB/$BiVO_4$ (PVB/BVO) nanocomposite film. This study describes the fabrication of PVB/BVO nanocomposite films using the solution casting technique. The effect of varying doses of gamma irradiation (0, 15, 30, 60, and 90) kGy on the structural, linear/nonlinear optical, dispersion, and optoelectrical characteristics of PVB/BVO nanocomposite films was then investigated. The pristine and irradiated PVB/BVO nanocomposite films were

evaluated via multiple techniques for characterization, which involves energy-dispersive X-ray spectroscopy (EDX), X-ray powder diffraction (XRD), Fourier transform-infrared spectroscopy (FT-IR), scanning electron microscopy (SEM), high resolution -transmission electron microscopy (HR-TEM), and ultra-violet/visible/near-infrared spectroscopy (UV–VIS–NIR). The remarkable characteristics exhibited by the proposed PVB/BVO polymeric composite films make them highly suitable for various applications in organic electronics, cut-off lasers, and optoelectronics.

2 Experimental

2.1 Materials and methods

Polyvinyl butyral (PVB), a pure powder produced by Sigma-Aldrich, USA, is one of the components used in this investigation. Vanadate pentoxide (V_2O_5) and bismuth oxide (Bi_2O_3) were purchased from Alfa-Aesar; tetrahydrofuran (THF, AR) and dioctyl phthalate (DOP, AR) were acquired from Nanjing Chemical Reagent Co., Ltd., Nanjing, China.

For pure BVO NPs, the present investigation successfully synthesized BVO using a solid-state reaction method. Bi_2O_3 and V_2O_5 were each weighted at a molar ratio 1:1 (Bi: V) as stoichiometric sources of Bi and V. The precursors were manually combined with a pestle and mortar to obtain a uniform composition and then ball milled for one hour. The resulting mixtures were calcined for four hours at 700 °C.

For the manufacture of the polymeric films, a polymer solution of 18% pure PVB was obtained by dissolving the required weight of PVB in THF; 2 ml of DOP was added as a plasticizer, and then the solution was magnetically stirred overnight at ambient temperature to produce a homogeneous solution. After that, BVO powder was dispersed in the prepared PVB solution at a concentration of 6 phr (hundred parts of resin), and the solution was agitated for 2 h at 60 °C using an ultrasound sonicator. Eventually, the resulting solutions were poured onto substrates made of glass utilizing an automatic film applicator apparatus. The polymeric film was allowed 48 h for drying at ambient temperature in a dark area. It was found that the average thickness of the dried coatings was approximately 100 μm. At the National Center for Radiation Research and Technology (NCRRT), Egyptian Atomic Energy Authority (EAEA), the PVB/BVO composite films were gamma-irradiated at various dosages (0, 15, 30, 60, and 90 kGy) using Co-60 γ-cell (Gamma Cell 220 Excel, MDS Nordion, Canada) at a dose rate of 0.8 kGy/h (Bekhit et al. 2021; Abdel Maksoud et al. 2021).

2.2 Characterization

The characterization of non-irradiated and irradiated PVB/BVO nanocomposite films has been conducted using various analytical tools. X-ray diffraction (XRD) techniques were utilized to evaluate the material's structural characteristics, utilizing a Shimadzu 6000 diffractometer configured in the Bragg–Brentano geometry. The conventional approach employed was the θ/2θ scanning technique. The radiation wavelength utilized is that of the CuKα line, which measures 0.15406 nm. The FTIR spectrometer (Nicolet iS10, USA) was utilized to evaluate the functional groups and complex formations of the PVB/BVO nanocomposite at various gamma doses. The measurements were taken within the wavenumber range of 4000–400 cm^{-1}. The examination of the size and shape of the BVO powder

produced was conducted through the utilization of a transmission electron microscope (TEM; JEM 2100, Jeol). The prepared BVO morphology was analyzed through a scanning electron microscope (SEM) with an accelerating voltage of 220 kV, JEOL JTEM-1230 model. Energy-dispersive X-ray spectroscopy (EDX) was conducted to illustrate the elemental composition and mapping images. The optical characteristics of the PVB/BVO nanocomposite films were evaluated through the determination of their absorption (Abs.), transmittance (T), and reflectance (R) using a UV-Visible-NIR spectrophotometer (JASCO V-570) with a wavelength range of 190–2500 nm.

3 Results and discussions

3.1 Structural studies

Figure 1 displays the EDX spectrum and elemental composition of BVO powder. The composition of the BVO powder is comprised of the chemical elements bismuth (Bi), vanadium (V), and oxygen (O). The non-existence of any foreign elements indicates the BVO sample's purity.

Figure 2(a,b) illustrates the SEM micrographs of the $BiVO_4$ powder sample. The morphology of $BiVO_4$ particles in their pure form exhibits a consistent plate-like structure, as depicted in Fig. 2(a, b). The grains are composed of large plates with an aggregated nature. Further, the microstructure features of the $BiVO_4$ powder have been obtained and examined using TEM and HR-TEM procedures to allow for a more comprehensive examination of their microscopic morphology. The transmission images in Fig. 2(c–d) reveals that the $BiVO_4$ powder has regular plate-like morphologies compatible with SEM investigations. Furthermore, the HR-TEM image allows for a detailed view of the surface of the magnified crystal grain, with a measured interplanar spacing of 0.310 nm, as depicted in Fig. 2(e). The resultant findings align perfectly with the interplanar distance of the (121) crystal plane, as stated in the $BiVO_4$ (JCPDS No. 14–0688)(Chen et al. 2019). Additional details regarding $BiVO_4$ powder were identified using selected area electron diffraction (SAED) ring patterns, as depicted in Fig. 2(f). The SAED rings corresponded to the planes of $BiVO_4$, which are a perfect fit for the phase structure of $BiVO_4$.

The X-ray diffraction (XRD) patterns of the pure PVB and $BiVO_4$ powder samples are depicted in Fig. 3(a). Notably, the formation of the amorphous structure of PVB is indicated by the broad diffraction peak ranging from $2\theta = 5$ to 25° (Maksoud et al. 2021; Lei et al. 2018). Further, the XRD pattern of $BiVO_4$ powder showed a single monoclinic phase (JCPDS card No. 14-0688) (Dabodiya et al. 2019; Guo et al. 2016). Besides, small peaks at 2θ =27.21°and 32.91° may be attributed to Bi_2O_3 as a residual of the synthesis process (Maksoud et al. 2021; Kassem et al. 2023). The crystallite size D of BVO powder was evaluated using the well-known Scherer equation(Holzwarth and Gibson 2011):

$$D = \frac{0.9\ x\ 0.15406\ (nm)}{\beta \cos\ (\theta)} \tag{1}$$

where 0.15406 nm is the wavelength (λ) of the used Cu K_α radiation. The calculated D of BVO powder was found to be 30.68 nm.

The presence of a butyral ring (C–O–C) in the PVB structure was verified through analysis of the FT-IR spectrum of the pure PVB film, which was conducted within the 4000–400 cm^{-1} range (Fig. 3(b)). The band observed at 3476 cm^{-1} in the FTIR spectrum

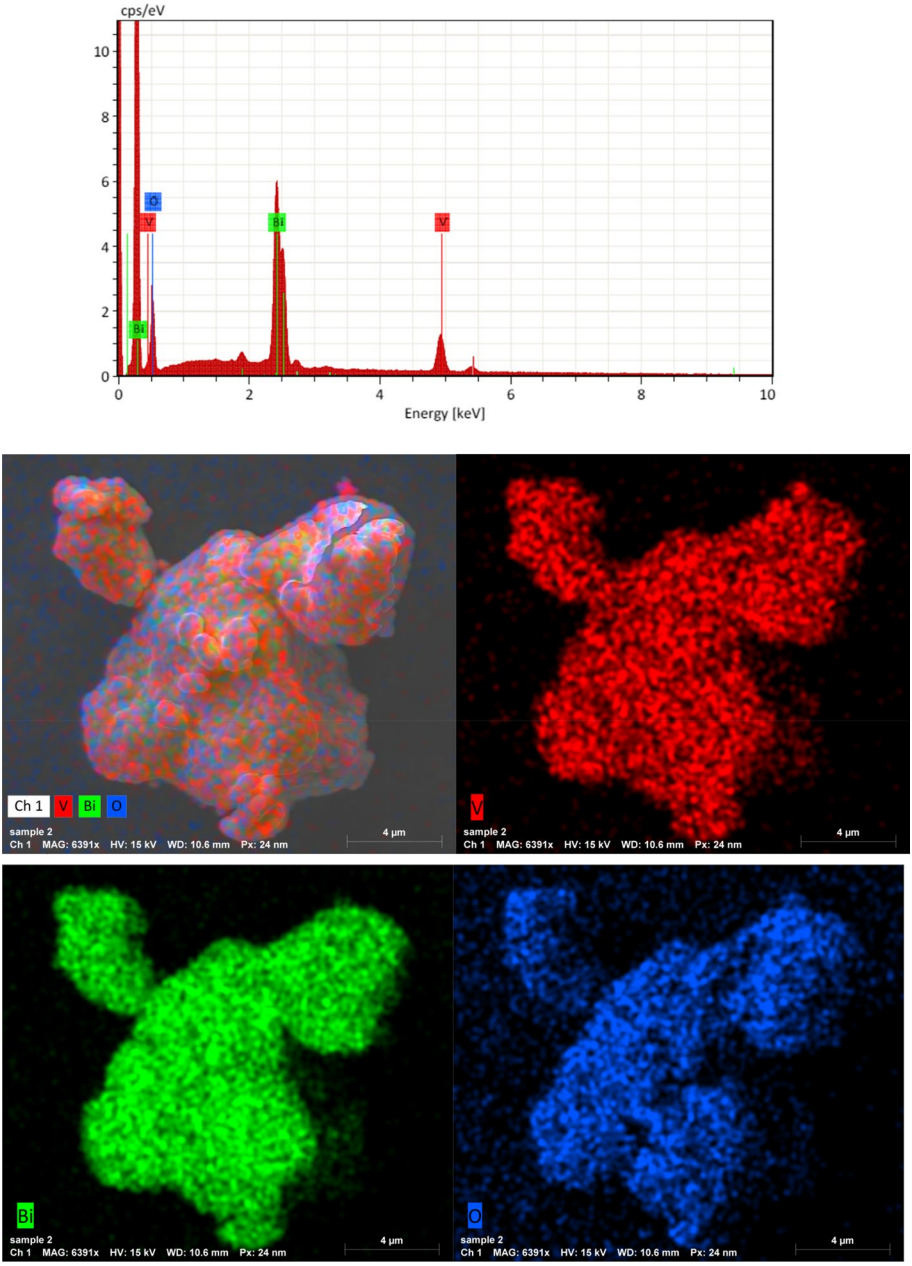

Fig. 1 EDX and elemental mapping images of $BiVO_4$ powder

corresponds to the O–H stretching. The bands noticed at 2945 and 2865 cm^{-1} correspond to aliphatic C–H stretching. The band noted at 1736 cm^{-1} corresponds to the C=O carbonyl group. The bands observed at 1429 and 1378 correspond to the bending of CH_2 and CH_3, respectively. The FTIR band watched at 1105 cm^{-1} is attributed to C–O–C stretching.

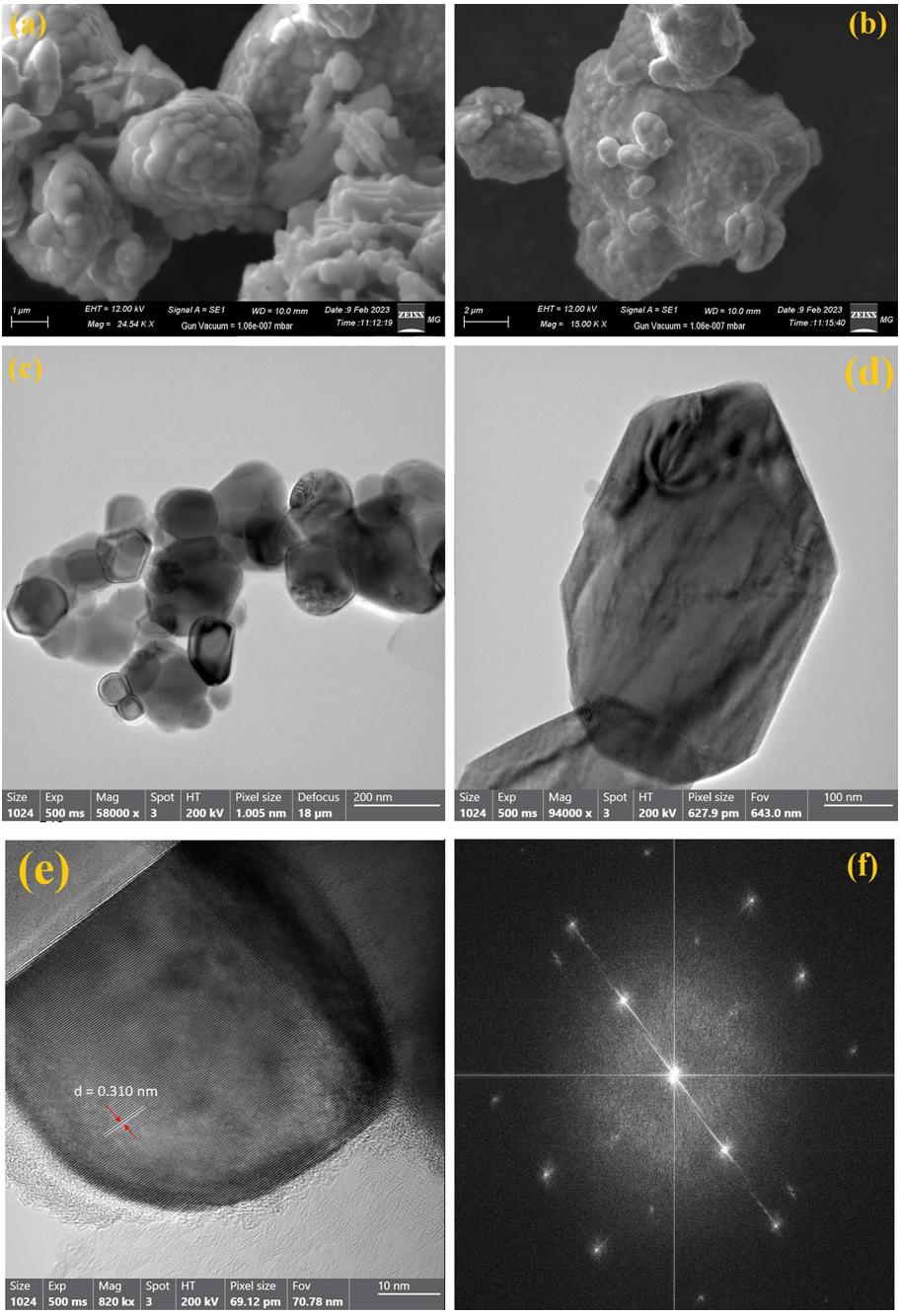

Fig. 2 **a** and **b** SEM, **c** & **d** TEM, **e** HR-TEM and **f** SAED images of $BiVO_4$ powder

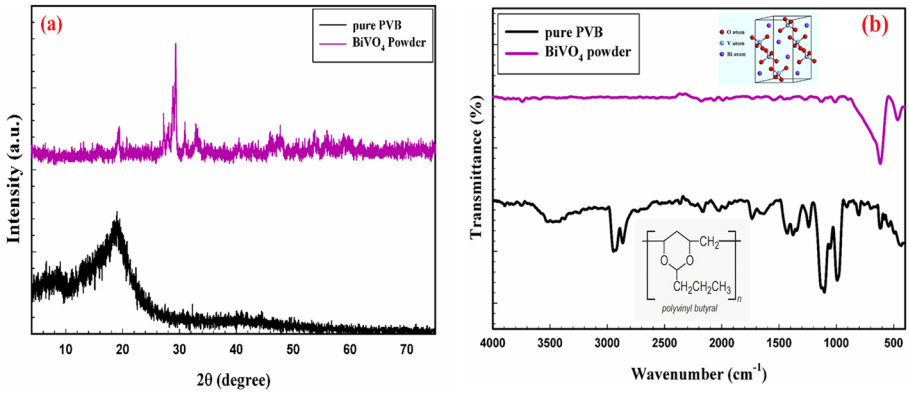

Fig. 3 **a** XRD patterns and **b** FTIR spectra of pure PVB and $BiVO_4$ powder

Furthermore, a band is noticed at a wavenumber of 993 cm^{-1} which can be attributed to the stretching of the C–O bond (Hajian et al. 2012; Mohammadian-Kohol et al. 2016). The purity of the produced material was validated by the FTIR spectrum of $BiVO_4$ powder, as shown in Fig. 3(b). A relatively small absorption band at 464 cm^{-1} attributable to the symmetric bending of VO_4^{-3} was also seen in the visible range, which matches the previously stated (Pookmanee et al. 2013). Also, the band at 616 cm^{-1} is attributed to Bi-O (Pookmanee et al. 2014; García-Pérez et al. 2012).

Fig. 4(a) depicts the XRD patterns of unirradiated and γ-irradiated PVB/BVO nanocomposite films. The presented figure demonstrates a correlation between the intensity of XRD peaks and the dosage of gamma rays. The intensity increases to a maximum value at 60 kGy. The evident phenomenon can be ascribed to the ionizing influence of gamma radiation, which reduces the intermolecular tension in the disordered regions, thus enhancing the polymer chains' mobility. This process enables the rearrangement of specific molecules.

Furthermore, exposure to γ radiation doses up to 90 kGy induces cross-linking, strengthening the bonds between $BiVO_4$ nanoparticles and the PVB polymer and disrupting the ordered regions within the nanocomposite (Nouh and Benthami 2019; Alhazime

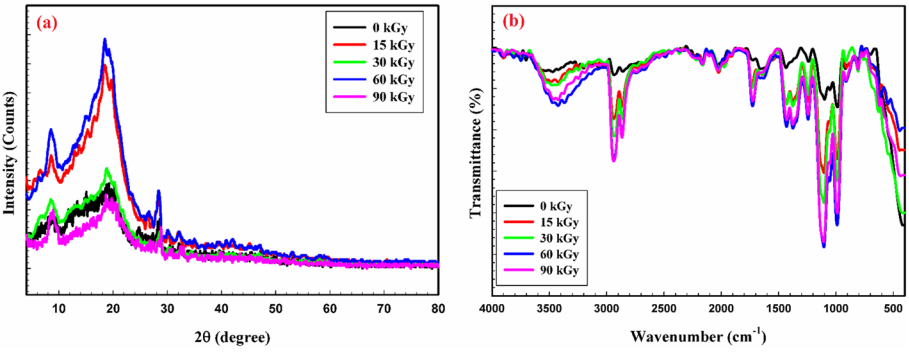

Fig. 4 **a** XRD patterns and **b** FTIR spectra of unirradiated and γ-irradiated PVB/BVO nanocomposite films

et al. 2021, 2020). This trend was observed in numerous studies (Alshahrani et al. 2021a, 2021b, Nouh and Benthami 2019; Alhazime et al. 2021, 2020). Whereas Alhazime et al. (Alhazime et al. 2020) have synthesized polyvinyl alcohol polyethylene glycol (PVA-PEG) film doped with Co_3O_4 NPs, and the film is exposed to γ-rays at a dosage range of 20–230 kGy. They observed the degradation of the composite upon exposure to γ-rays at a dose range of 20–60 kGy. Besides, they reported that cross-linking the series of irradiated films was observed within a range of gamma-ray doses from 60 to 180 kGy. Additionally, the intensity rises again at 180 kGy and up to 230 kGy due to degradation.

The effects of gamma radiation on the structural properties of PVB/ $BiVO_4$ nanocomposite films have been demonstrated through FTIR spectroscopy. The induced modifications were assessed by examining the changes in band intensity associated with each functional group. The absorbance values of the un-irradiated and irradiated films are presented in Fig. 4(b). Un-irradiated PVB/$BiVO_4$ nanocomposite film displayed FTIR bands corresponding to pure PVB polymer and those related to the $BiVO_4$ nanofiller. The spectral analysis of PVB/$BiVO_4$ nanocomposite film (0 kGy), depicted in Fig. 4(b), reveals significant alterations and impacts on the functional groups within the PVB matrix upon incorporating $BiVO_4$ NPs. The addition of $BiVO_4$ NPs reduces the hydroxyl group's intensity and broadness. The spectral features of CH_2 stretching vibration at 1435 cm^{-1} and the C–O–C group at 1099 cm^{-1} increase their broadness after filling $BiVO_4$ NPs, accompanied by a corresponding reduction in their intensity. This implies a strong interaction between the PVB matrix and $BiVO_4$ NPs (Abdelghany et al. 2016). As the γ-irradiation dose rises from 15 to 60 kGy, the strength of the CH_2 stretching band expands, but its broadness reduces, while the intensity of absorption bands in the 1500–800 cm^{-1} area declines significantly. However, with less distortion, the shape of the carbonyl group appears more ordered. This indicates that structural rearrangements in the chain of PVB/$BiVO_4$ nanocomposite films exist in this dose rate area, as validated by XRD measurements. Upon exposure to incremental γ-irradiation up to 90 kGy, a reduction in the intensity and broadness of the hydroxyl group was observed. The spectral bands associated with aliphatic C–H stretching exhibit variability in response to changes in gamma radiation doses. The observed trend can be attributed to the rearrangement and cross-linking processes induced by exposure to significant doses of radiation, leading to noticeable changes in the amorphous regions within the PVB polymeric matrix (Alhazime et al. 2020; Abdelghany et al. 2016).

3.2 Linear optical properties of pristine and γ-irradiated PVB/BVO nanocomposite films

3.2.1 Spectral behavior of the transmittance (T)

Investigating materials' optical characteristics and establishing their optical constants is essential to know the electrical and band structures for developing optoelectronic devices. Figure 5 displays the transmittance, T (λ), of the PVB/BVO nanocomposite films before and after treatment with γ-rays as a function of wavelength in the range (190–2500) nm. Furthermore, the non-irradiated and γ-rays-treated PVB/BVO nanocomposite films demonstrate an absorption peak at nearly 201 nm and an absorption band at 271 nm. The observed bands are suggestive of the host polymer electronic transitions of $\pi \rightarrow \pi^*$ and $n \rightarrow \pi^*$, respectively (Badawi et al. 2022; Alharthi and Badawi 2022). Based on the results presented in Fig. 5, it can be observed that the transmittance T (λ) altered as a consequence of the gamma radiation treatment process.

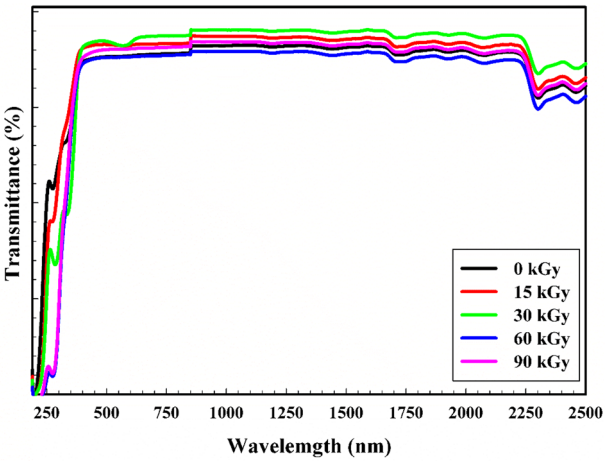

Fig. 5 The transmittance T (λ) of unirradiated and γ-irradiated PVB/BVO nanocomposite films

Additionally, there is a redshift towards longer wavelengths as the gamma radiation dose increases from 15 to 90 kGy. The observed shift in transmittance indicates a related reduction in the optical bandgap of the composite films, which can be attributed to the γ-radiation treatment. Furthermore, distinct redshifts are observed in the cut-off edges of the γ-radiation treated PVB/BVO nanocomposite films compared to the untreated composite film with γ-radiation. The wide range observed in the shift of the transmittance and cut-off edges of the prepared PVB/BVO nanocomposite films suggests their potential uses for optical devices (Alshahrani et al. 2021a, 2021b; Alharthi and Badawi 2022).

3.2.2 Optical energy gap and Urbach tail

The assessment of the energy gap, Eg, is an essential variable for solid materials in the context of optoelectronic devices and the design of novel solar cells. The estimation of the absorption coefficient (α) for PVB/BVO nanocomposite films can be achieved through the utilization of measured values of transmittance (T) and reflectance (R) within the wavelength range of 190–2500 nm for both pristine and γ-irradiated PVB/BVO nanocomposite films. This calculation can be performed using an equation as follows (Sell et al. 1974).

$$\boldsymbol{\alpha} = \left(\frac{1}{\boldsymbol{d}}\right)\boldsymbol{ln}\left(\frac{(1-\boldsymbol{R})^2}{2\boldsymbol{T}} + \sqrt{\frac{(1-\boldsymbol{R})^4}{4\boldsymbol{T}^2} + \boldsymbol{R}^2}\right), \tag{2}$$

The linear and nonlinear optical characteristics of the PVB/BVO nanocomposite films were determined based on measurements of transmittance T(λ) and absorbance A(λ). The direct and indirect optical bandgap (E_g) of the PVB/BVO nanocomposite films, both pristine and irradiated, have been assessed using Tauc's relation (Krumhansl 1957).

$$\boldsymbol{\alpha h\nu} = \boldsymbol{B}(\boldsymbol{h\nu} - \boldsymbol{E_g})^t \tag{3}$$

As mentioned earlier, the equation involves a constant denoted as B, the optical absorption represented by α, and the energy of the incident photons indicated as hυ. The t parameter is associated with the electronic transition type noticed in the PVB/BVO nanocomposite films. The permissible direct transitions are characterized by a value of

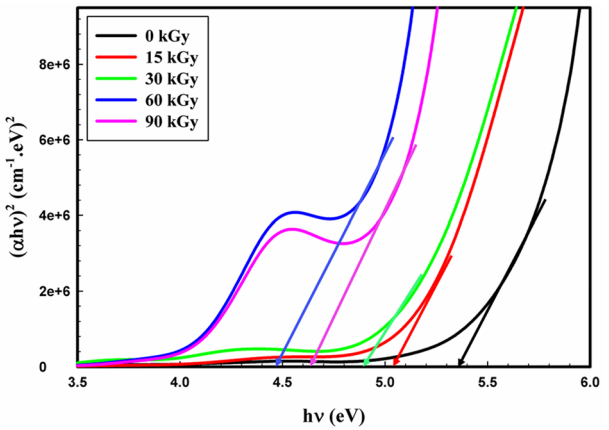

Fig. 6 $(\alpha h\nu)^2$ versus hν of unirradiated and γ-irradiated PVB/BVO nanocomposite films

1/2 for t, while the acceptable indirect transitions are marked by 2 for t. The direct (Eg) energy gap values of PVB/BVO nanocomposite films were estimated from Fig. 6 by extrapolating the line slice until the absorption reached zero on the y-axis. The findings of the optical band gap in the current study have been assembled in Table 1, revealing a discernible trend in the behavior of Eg. Specifically, it is observed that Eg decreases from 5.33 to 4.47 eV as the gamma radiation dose increases from 0 to 60 kGy. Subsequently, Eg increases at a gamma ray dose of 90 kGy to reach 4.67 eV. The decrease in the energy bandgap (Eg) can be attributed to the impact of gamma radiation on the chemical bonding configuration between PVB chains and $BiVO_4$ NPs. This effect is significant enough to generate localized states within the highest occupied molecular orbital (HOMO) and lowest unoccupied molecular orbital (LUMO) band edges, which reduces the accessibility of energy transitions (Devi et al. 2002; Zidan 2003). Thus, in the current instance, the strengthened conjugation between $BiVO_4$ NPs and unsaturated bonds of PVB (as evidenced by the FTIR analysis) leads to a significant decrease in the energy gap due to gamma irradiation (Eisa et al. 2011; Bhat et al. 2005). The extraordinary improvement in the optical band gap value of PVB/BVO nanocomposite film at 90 kGy suggests that gamma radiation causes cross-linking of the PVB/BVO nanocomposite film; this type of behavior was additionally apparent in XRD patterns (Nouh et al. 2018).

The relationship between the optical energy gap (Eg) values and the number of carbon atoms per cluster (N) in the PVB/BVO nanocomposite films can be established as follows (Fink et al. 1995; Reheem et al. 2016):

Table 1 The optical parameters of unirradiated and γ-irradiated PVB/$BiVO_4$ nanocomposite films

Sample	Eg (eV)	*N*	EU (eV)
0 kGy	5.33	41.41	2.62
15 kGy	4.94	48.20	2.62
30 kGy	4.83	50.43	3.32
60 kGy	4.47	58.88	4.07
90 kGy	4.67	53.94	3.00

$$E_g = \frac{34.3}{\sqrt{N}} \tag{4}$$

As shown in Table 1, as the optical band gap decreases, the number of carbon atoms in each cluster (N) grows according to rising gamma irradiation.

The absorption coefficient curve exhibits an exponential section called the Urbach tail close to the optical band edge. The PVB/BVO nanocomposite films' exponential dependency on photon energy (hυ) suggests that they obey Urbach's equation.

The present study investigated the defects generated in PVB/BVO nanocomposite films as a result of the irradiation process via a focus on the Urbach energy (E_U) (Urbach 1953):

$$\alpha = \alpha_0 \, exp\left(h\nu / E_U\right) \tag{5}$$

The natural logarithm of the absorption coefficient (ln α) has been plotted as a function of photon energy hυ for the examined PVB/BVO nanocomposite films to demonstrate this dependency, as can be seen in Fig. 7. Table 1 shows Urbach's energy (E_U) computed and listed values. This data demonstrates that Eu increases from 2.62 eV for the pristine PVB/BVO nanocomposite film to 4.07 eV for the irradiated PVB/BVO nanocomposite film with 60 kGy. The irradiation via gamma rays boosts the number of traps in PVB/BVO nanocomposite films, which causes fewer efficient energy transitions and an associated decrease in the optical energy gap (El-Malawy et al. 2021). In other words, the considerable variation in the band gap can be attributed to forming more free radicals and active products as a direct result of the interaction of energetic photons with the composite network forming scission and cross-linking. Furthermore, a significant reduction in Urbach's energy (E_U) was noticed at a dose of 90 kGy (3.00 eV) which can be attributed to the cross-linking process (Alhazime et al. 2021).

3.2.3 Refractive index and extinction coefficient

The refractive index (n) is a crucial parameter in optical physics that describes the electronic polarization of ions in a substance. It plays a significant role in developing spectral dispersion tools and optical communication (Li et al. 2022).

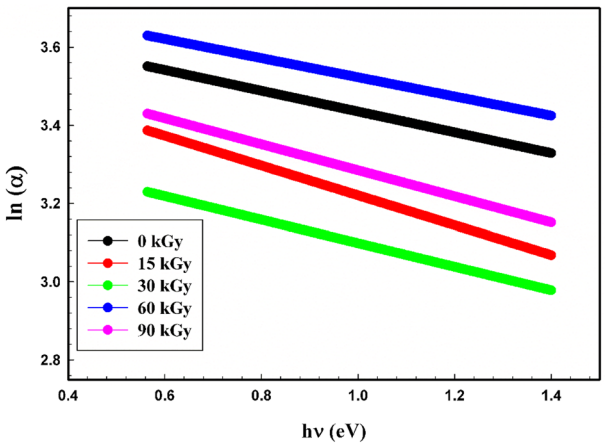

Fig. 7 ln (α) vs. photon energy for unirradiated and γ-irradiated PVB/BVO nanocomposite films under different doses of γ-rays irradiation

In this research, we derived the refractive index (n) and the extinction coefficient (k) from the references stated in (Sell et al. 1974; Taha 2019; Reyes-Coronado et al. 2018; Lee et al. 2003; Zeyada et al. 2012; El-Ghamaz et al. 2017):

$$n = \frac{1+R}{1-R} + \sqrt{\frac{4R}{(1-R)^2} - k^2} \tag{6}$$

$$k = \frac{\alpha\lambda}{4\pi} \tag{7}$$

Figure 8 illustrates the variation in n throughout different sets of λ for all PVB/BVO nanocomposite samples. The dispersion relation revealed a gradual decrease in the value of n as λ and gamma-ray doses increased, which can be attributed to internal modifications to the structure and inter-atomic forces (Abdelghany et al. 2016). The highest refractive index of the pristine PVB/BVO nanocomposite film is 2.02, which is greater than the published value for 6wt% B_2O_3@$BaZrO_3$ ions doped PVB (Maksoud et al. 2021). A high refractive index value suggests that the film is dense, causing a decline in inter-atomic space. Upon exposure to gamma-irradiation at a dosage of 60 kGy, the polymeric matrix of the PVB/BVO nanocomposite film undergoes structural rearrangement, resulting in a reduction in the total amount of non-bridging oxygen (NBO) bonds due to the degradation process. In addition, exposing the PVB/BVO nanocomposite films to high doses of gamma irradiation (specifically, at 90 kGy) has been observed to improve the number of inter-chain interactions. This leads to alterations in the distribution of molecular weight and packing density, subsequently increasing the value of n as the irradiation dose is increased(Abdelghany et al. 2016).

Once gamma-irradiation doses grow, the extinction coefficient (k) improves, then decreases in the case of 90 kGy, as seen in Fig. 9. Furthermore, chain scission and cross-linking may cause changes in chain rearrangement, which can lead to significant changes in the extinction coefficient (k).

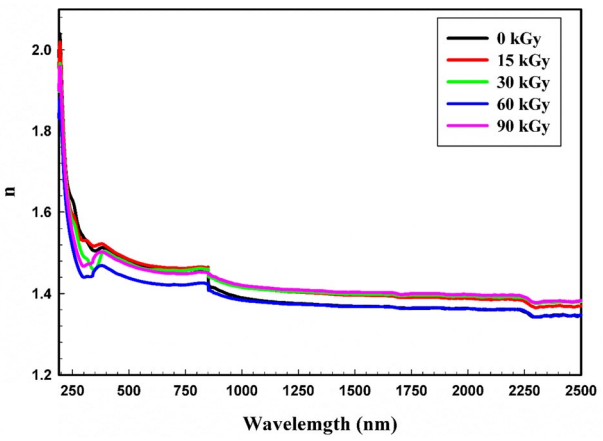

Fig. 8 The refractive index (n) vs. wavelength (λ) for unirradiated and γ-irradiated PVB/BVO nanocomposite films under different doses of γ-rays irradiation

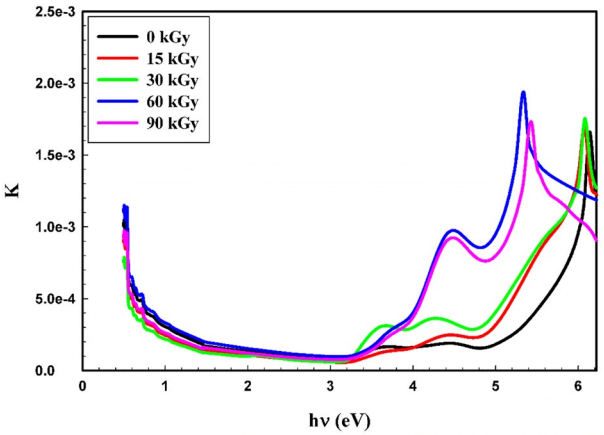

Fig. 9 The relation between the k coefficient against hυ for unirradiated and γ-irradiated PVB/BVO nanocomposite films under different doses of γ-rays irradiation

3.2.4 Dispersion constants and the dielectric constants

The Wemple and DiDomenico relationship can be utilized to express the oscillator energy (E_o) and dispersion energy (E_d) of the PVB/BVO nanocomposite films by adopting the single oscillator model (Wemple and DiDomenico 1971).

$$\frac{1}{n^2-1}=\frac{E_o}{E_d}-\frac{1}{E_oE_d}(h\nu)^2 \tag{8}$$

The meaning of oscillator energy E_o is related to the average excitation energy required to cause electronic transitions. In contrast, the dispersion energy, denoted by the E_d, is related to the strength of the interband transitions in the optical spectrum and corresponds with many aspects of the ordered structure of the material, in addition to the effective oscillator energy (Taha 2019). Both unirradiated and irradiated PVB/BVO nanocomposite films were measured for their oscillator energy E_o and their dispersion energy E_d under different doses of γ-rays irradiation can potentially be estimated from the intersection and slope of

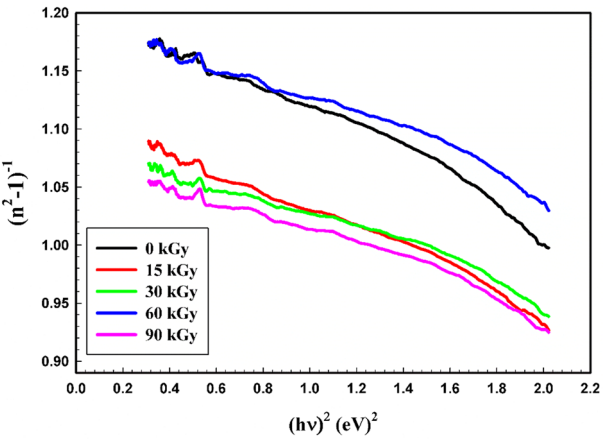

Fig. 10 $(n^2-1)^{-1}$ against $(h\nu)^2$ graphs of PVB/BVO nanocomposite films

Table 2 Values of dispersion parameters and dielectric constants for unirradiated and γ-irradiated PVB/BVO nanocomposite films

Sample	E_0 (eV)	E_d (eV)	n_o	f (eV)^2	ε_s	N/m* × 10^{55} (Kg^{-1} m^{-3})	ε_∞
0 kGy	3.6834	3.0593	1.3530	11.2689	1.8306	1.6173	1.908
15 kGy	3.6899	3.3212	1.3784	12.2549	1.9001	1.9805	1.990
30 kGy	4.1981	3.8657	1.3859	16.2285	1.9208	1.4099	1.987
60 kGy	4.1235	3.4506	1.3553	14.2288	1.8368	1.3866	1.901
90 kGy	4.1122	3.8253	1.3893	15.7307	1.9302	1.4369	2.000

the smoothly fitted lines over a plot of $1/(n^2\text{-}1)$ against $(h\upsilon)^2$, as illustrated in Fig. 10 and displayed in Table 2.

The formula for calculating the static refractive index n_0, which pertains to $h\upsilon = $ zero, is determined using the following equation(Taha 2019).

$$n_o = \sqrt{1 + \frac{E_d}{E_0}} \tag{9}$$

The computation of the static dielectric constant can be determined by utilizing the static refractive index, which is expressed as $\varepsilon_s = n_o^2$ (Alshahrani et al. 2021b). In addition, the values of E_0 and E_d are shown in Table 2**,** along with the definition of optical oscillator strengths (f) for optical transitions based on the absorbed energy of a photon through the electron between the initial and final states. This absorption of a photon has a relationship with E_0 and E_d, and it may be stated as $f = E_o E_d$ (Taha 2019). Upon irradiation with gamma rays, the oscillator and the dispersion energy both increased, matching the behavior of the optical parameters. This typically indicates that defects are dispersed throughout the PVB matrix due to gamma rays altering the electrical structure of the PVB composite molecule.

The dielectric constant plays a crucial role in establishing the relationship between the electron transitions occurring between bands in materials and their fundamental structural characteristics (Emara et al. 2019). The nonlinear optical properties of materials are influenced by the dielectric constant, which is responsible for the polarizability of the material (Sahoo and Naik 2022). The dielectric constants can be determined using the absolute magnitudes of the refractive and extinction coefficients. Using the following equations, the real part of the dielectric constant, ε_r, and the imaginary portion of the dielectric constant, ε_i, can be derived (Reyes-Coronado et al. 2018; Lee et al. 2003).

$$\varepsilon_r = n^2 - k^2, \varepsilon_i = 2nk \tag{10}$$

The present study displays the values of the dielectric constants (ε_r & ε_i) of PVB/BVO nanocomposite films before and after exposure to γ-irradiation as a function of photon energy hυ, as shown in Fig. 11(a,b). We observed that as γ-rays energy increased, the real dielectric constant (ε_r) decreased while the imaginary dielectric constant (ε_i) increased. In addition, the response of these constants changes when the gamma radiation reaches 90 kGy. This phenomenon can be attributed to the degradation and cross-linking mechanisms that were previously discussed (Alshahrani et al. 2021b).

The high-frequency dielectric constant ε_∞ can be identified by evaluating the real part of the dielectric constant ε_r, as expressed by the following equation (Palik 1985; Aly 2023):

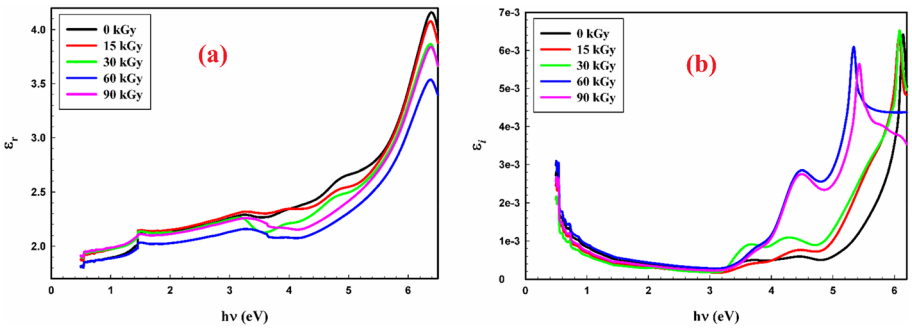

Fig. 11 **a** real part and **b** imaginary part of the dielectric constant for unirradiated and γ-irradiated PVB/BVO nanocomposite films

$$n^2 - k^2 = \varepsilon_\infty - \left(\frac{e^2}{4\pi^2\varepsilon_0 c^2}\right)\left(\frac{N}{m^*}\right)\lambda^2 \tag{11}$$

The above formula involves various physical parameters such as the charge of the electron denoted by 'e', the free charge-carrier concentration represented by 'N', the permittivity of the free space denoted by 'ε_0', the effective mass of the charge carriers in kilograms represented by 'm*', and the velocity of light in vacuum represented by 'c'.

The values of the high-frequency dielectric constant ε_∞ and the ratio of the concentration of free carrier ions to the effective mass (N/m*) can be driven through computation of the intercept and slope of the linear part in the plots of ε_r versus λ^2, as depicted in Fig. 12 and the values are listed in Table 2. It can be observed that exposure to gamma radiation has a significant impact on the ratio (N/m*) and the high-frequency dielectric constant ε_∞.

Oscillator strength is a dimensionless variable used in spectroscopy to represent the probability of electromagnetic radiation absorption or emission during transitions between atomic or molecular energy levels. The single oscillator model can be utilized to derive the average oscillator wavelength (λ_0), oscillator strength (S_0), and the refractive index at elongated

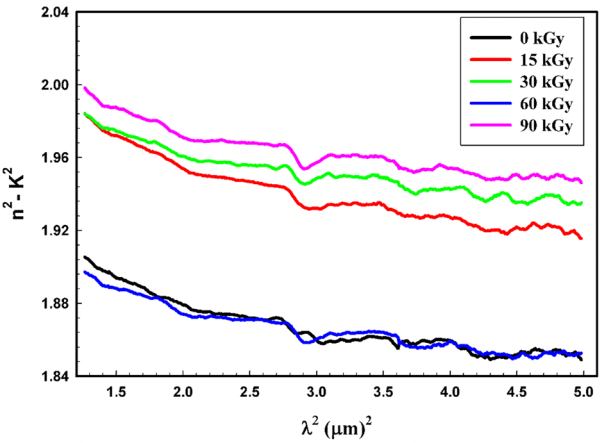

Fig. 12 The relation between (n^2–k^2) and λ^2 for unirradiated and γ-irradiated PVB/BVO nanocomposite films

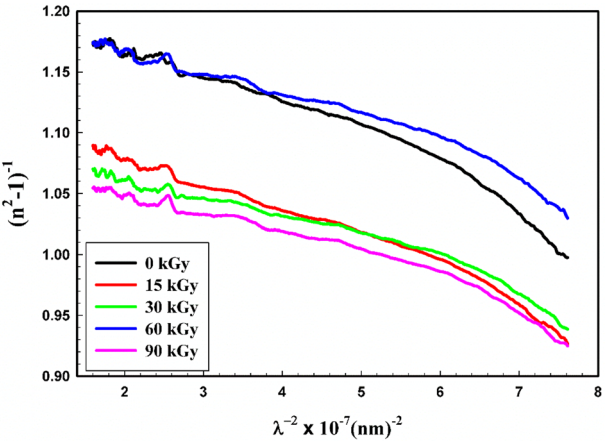

Fig. 13 The relation between $(n^2-1)^{-1}$ and λ^{-2} for unirradiated and γ-irradiated PVB/BVO nanocomposite films

wavelength (n_∞) parameters of PVB/BVO nanocomposite films. This can be achieved through linear regression of $(n^2\text{-}1)^{-1}$ against λ^{-2}, as illustrated in Fig. 13 (Taha 2019).

$$\frac{1}{n^2-1} = \left(\frac{1}{S_O \lambda_0^2}\right) - \left(\frac{1}{S_0}\right)\lambda^{-2} \tag{12}$$

$$n_\infty^2 - 1 = S_O \lambda_0^2 \tag{13}$$

Table 3 presents the λ_0 and S_0 values. The results indicate a notable variation in both λ_0 and S_0 parameters after that gamma exposure to radiation.

3.3 Nonlinear optical properties

Organic nonlinear optical (NLO) materials have garnered a great deal of research attention due to the enormous potential they have for a wide range of uses, including developing cutting-edge, optoelectronic devices, on-chip optical communication, microlasers, illumination, displaying, and biological sensing (Tian et al. 2023). The phenomenon of nonlinearity appears in the system when it is subjected to an energy of significant intensity, resulting in a modification of its inherent characteristics. Nonlinear optics refers to the optical response of a material to properties, including the phase or path of light that penetrates it, polarization, and frequency (Alosabi et al. 2023).

The linear optical susceptibility, $\chi^{(1)}$, third-order nonlinear optical susceptibility, $\chi^{(3)}$, and nonlinear refractive index, n_2, of PVB/BVO nanocomposite films is a prerequisite for their multiple uses, including capacity for communication. Consequently, the present study concentrates on determining the relationships between $\chi^{(3)}$ and interband transitions, as well as a numerical formula for deriving the third-order susceptibility of the films as a function of gamma dosages. The following equations have been applied for the computation of the nonlinear optical parameters for PVB/BVO nanocomposite films (Taha 2019; Frumar et al. 2003; Ticha and Tichy 2002a):

$$\chi^{(1)} = E_d / 4\pi E_0 \tag{14}$$

Table 3 Values of oscillator strength, nonlinear and optoelectronics parameters for unirradiated and γ-irradiated PVB/BVO nanocomposite films

Sample	$So \times 10^{-6}$ nm^{-2}	λo (nm)	n_∞	$\chi^{(1)}$	$\chi^{(3)} \times 10^{-15}$ e.s.u	$n_2 \times 10^{-15}$ e.s.u	τ fS	$\omega p \times 10^{14}$ Hz	$\mu_{opt.} \times 10^{-3}$ ($C.S.kg^{-1}$)
0 kGy	4.1169	446.39	1.3492	0.0661	3.2455	90.467	0.536	2.6610	9.43
15 kGy	4.4563	446.62	1.3744	0.0716	4.4764	122.474	0.739	2.8620	12.99
30 kGy	5.9242	392.45	1.3829	0.0732	4.9030	133.422	0.629	2.4666	11.06
60 kGy	5.1840	399.77	1.3522	0.0666	3.3444	93.064	0.426	2.4962	7.51
90 kGy	5.7471	400.46	1.3862	0.0740	5.1068	138.628	0.517	2.5595	9.11

$$\chi^{(3)} = 6.82 \times 10^{-15} (E_d/E_0)^4 \tag{15}$$

$$n_2 = 12\pi\chi^{(3)}/n_0 \tag{16}$$

Notably, the optical nonlinearity of an optical material occurs during the polarization process upon exposure to an electric field. The results indicate that the values of $\chi^{(1)}$, $\chi^{(3)}$, and nonlinear refractive index (n_2) exhibited an increase with increasing gamma doses, as illustrated in Table 3. It can be seen that the $\chi^{(1)}$ increases from 0.0661 to 0.0740, and $\chi^{(3)}$ rises from 3.2455 to 5.1068×10^{-15} esu with increasing gamma radiation doses. While the n_2 enhanced from 90.467 to 138.628×10^{-15} esu. In another study (Badawi et al. 2022) has examined the effect of gamma irradiation on the structural, linear, and nonlinear optical characteristics of a PVA/graphene composite containing lead oxide. It is found that the $\chi^{(1)}$ increases from 0.19 to 0.45 and $\chi^{(3)}$ rises from 2.25 to 6.76×10^{-12} esu esu as a result of the increase in γ-irradiation. The value of n_2 rises from 5.21 to 9.95×10^{-11} esu as the γ-irradiation dose is increased from 0 to 250 kGy.

3.4 Opto-electrical properties

The Drude model has developed relationships between the imaginary and real parts of the dielectric constants, facilitating the computation of several optoelectrical parameters, including relaxation time, τ, the plasma frequency, ω_p, optical mobility $\mu_{opt.}$, and optical resistivity ρ_{opt}.

The relationship between the real part of the dielectric constant, ε_r, the high-frequency dielectric constant, ε_∞, and the plasma frequency, ω_p, is represented as follows (Abou Hussein et al. 2021; El-Bana and Fouad 2017):

$$\varepsilon_r = \varepsilon_\infty - \frac{\omega_p^2}{\omega^2} \tag{17}$$

Using the slopes of the plots between ε_r and $1/\omega^2$ (see Fig. 14), the values of ω_p are estimated for the studied compositions. The extracted values of ω_p for the investigated

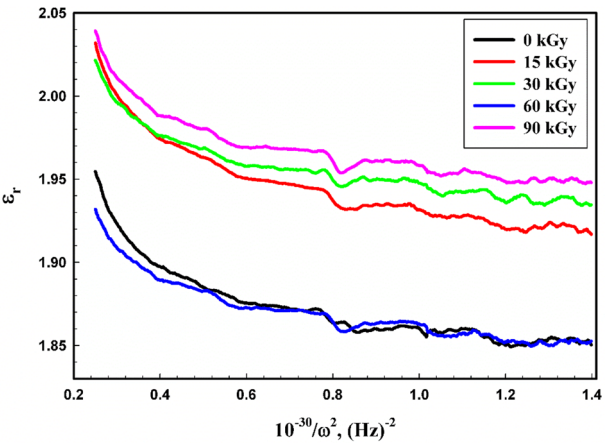

Fig. 14 Variation of the real dielectric constant concerning $1/\omega^2$ for unirradiated and γ-irradiated PVB/BVO nanocomposite films

compositions are listed in Table 3, and it has been shown that gamma irradiation significantly impacts the variation of ω_p with increasing gamma dosages.

Additionally, the relaxation time, τ, can also be computed based on the relationship between the imaginary dielectric constant and wavelength utilizing the following formula (Aly 2023):

$$\varepsilon_i = \frac{1}{8\pi^3\varepsilon_0}\left(\frac{e^2}{c^3}\right)\left(\frac{N}{m*}\right)\frac{1}{\tau}\lambda^3 \tag{18}$$

The reciprocal straight-line slope in the relation between ε_i and λ^3 (Fig. 15) can be used to estimate the relaxation time τ. The relaxation time values for the investigated compositions are listed in Table 3. The relaxation time values ranged between 0.426 fS and 0.739 fS as the γ–rays doses varied.

By employing the values of τ, the following relations were used for the calculation of optical mobility μ_{opt} (Ticha and Tichy 2002b; Saadeddin et al. 2007):

$$\mu_{opt} = \frac{e\tau}{m_o} \tag{19}$$

The optical mobility μ_{opt} decreased from $9.43\times\ 10^{-3}$ C.S./kg for um-irradiated PVB/BVO nanocomposite film to $7.51\times\ 10^{-3}$ C.S./kg for irradiated PVB/BVO nanocomposite film at 60 kGy before increasing again to $9.11\times\ 10^{-3}$ C.S./kg at 90 kGy.

Charge carriers, transported by the alternating electric field of the incoming electromagnetic waves, are responsible for optical conductivity. Optical conductivity ($\boldsymbol{\sigma_{opt}}$) is the main factor that elucidates the light response of a material (Taha 2019). The optical conductivity ($\sigma_{opt.}$) can be derived from the next relation (Sell et al. 1974; Taha 2019; Reyes-Coronado et al. 2018; Lee et al. 2003; Zeyada et al. 2012; El-Ghamaz et al. 2017):

$$\sigma_{opt} = nc\alpha/4\pi \tag{20}$$

C denotes the speed of light in a vacuum.

Figure 16 demonstrates a correlation between the optical conductivity ($\boldsymbol{\sigma_{opt}}$) and photon energy of the PVB/BVO nanocomposite films. The optical conductivity increases in response to alterations in gamma radiation dosages. The effect occurs as the bandgap

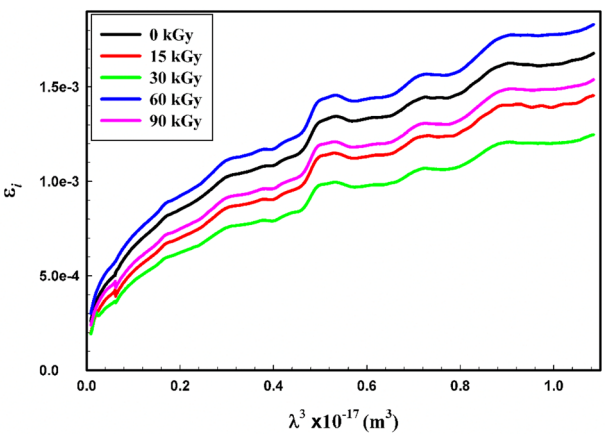

Fig. 15 The relationship between ε_i and λ^3 for unirradiated and γ-irradiated PVB/BVO nanocomposite films

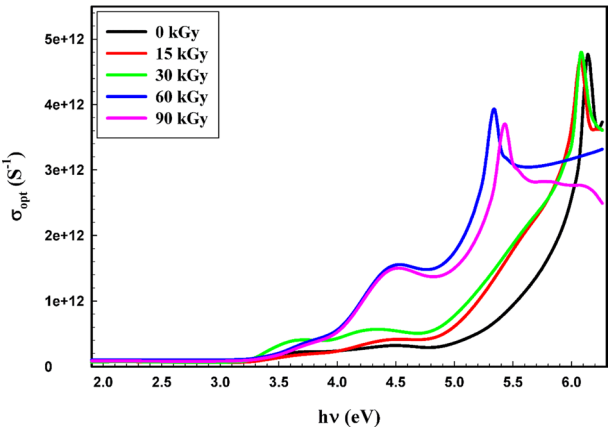

Fig. 16 The optical conductivity (σ_{opt}) Vs. photon energy for unirradiated and γ-irradiated PVB/BVO nanocomposite films under different doses of γ-rays irradiation

decreases, allowing for enhanced conductivity due to the facilitated movement of electrons from the valence band to the conduction bands (Morad et al. 2020). In our study, at hυ = 4.5 eV, the optical conductivity (σ_{opt}) increased from 3.21 × 10^{11} S^{-1} to 1.54×10^{12} S^{-1} as gamma radiation doses increased from 0kGy to 60 kGy and then decreased to 1.49 × 10^{12} S^{-1} at 90 kGy. In another study, the optical conductivity (σ_{opt}) increased from 1.51×10^{11} S^{-1} to 4.54 × 10^{11} S^{-1} as gamma radiation doses increased from 0 kGy to 250 kGy, as presented in recent research by Badawi et al. (Badawi et al. 2022)

4 Conclusions

The present study investigates the impact of gamma irradiation on the structural, dispersion, linear/nonlinear optical, and optoelectrical properties of PVB/$BiVO_4$ nanocomposite films. The nanocomposite films were exposed to varying doses of gamma radiation (0, 15, 30, 60, and 90 kGy), and the effects were analyzed.

XRD and FT-IR analyses provide information regarding the effect of gamma radiation on the degree of crystallinity of the PVB/BVO films. Dielectric constants and other associated parameters were computed using the estimated refractive index and extinction coefficient values. The compositional optical behavior dependence on the gamma irradiation dosages was studied by estimating the plasma frequency, relaxation time, and optical mobility. The energy gap varied between 4.47 and 5.33 eV, while the Urbach energy increased from 2.62 to 4.07 eV. The oscillator energy improves from 3.68 eV for the unirradiated PVB/BVO film to 4.19 eV for the 30 kGy-irradiated PVB/BVO nanocomposite film before decreasing to 4.11 eV for the 90 kGy-irradiated PVB/BVO nanocomposite film. Additionally, the dispersion energy ranged from 3.05 to 3.86 eV, and the static dielectric constant increased from 1.83 for the virgin PVB/BVO nanocomposite film to 1.93 at 90 kGy. The PVB/$BiVO_4$ nanocomposite films may suit organic light-emitting diodes, organic solar cells, and other flexible organic electronic devices based on linear/nonlinear characteristics, dispersion parameters, and optical conductivity.

Author contribution M. I. A. AM: Data curation, Investigation, Methodology, Writing—original draft, Writing—review & editing. RAF: Data curation, Investigation, Methodology, Writing—original draft, Writing—review & editing. Said M. K: Data curation, Investigation, Methodology, Writing—original draft,

Writing—review & editing. A. S. A: Data curation, Investigation, Methodology, Writing—original draft, Writing—review & editing.

Funding Open access funding provided by The Science, Technology & Innovation Funding Authority (STDF) in cooperation with The Egyptian Knowledge Bank (EKB). None.

Data availability All data generated or analysed during this study are included in this published article.

Declarations

Competing interests The authors declare no competing interests.

Consent to participate Not applicable.

Consent to publish Not applicable.

Ethical approval Not required.

References

Abdel Maksoud, M.I., Awed, A.S., Sokary, R., Bekhit, M.: Effect of gamma irradiation on the free-standing polyvinyl alcohol/chitosan/Ag nanocomposite films: insights on the structure, optical, and dispersion properties. Appl. Phys. a. **127**, 1–1 (2021)

Abdel Maksoud, M.I., Bekhit, M., Waly, A.L., Awed, A.S.: Optical and dielectric properties of polymer nanocomposite based on PVC matrix and Cu/Cu_2 O nanorods synthesized by gamma irradiation for energy storage applications. Phys. E Low-Dimension. Syst. Nanostruct. **148**, 115661 (2023)

Abdelghany, A.M., Abdelrazek, E.M., Badr, S.I., Morsi, M.A.: Effect of gamma-irradiation on (PEO/PVP)/Au nanocomposite: Materials for electrochemical and optical applications. Mater. Des. **97**, 532–543 (2016)

Abou Hussein, E.M., Maksoud, M.A., Fahim, R.A., Awed, A.S.: Unveiling the gamma irradiation effects on linear and nonlinear optical properties of CeO2–Na2O–SrO–B2O3 glass. Opt. Mater. **1**(114), 111007 (2021)

Alharthi, S.S., Badawi, A.: Tailoring the linear and nonlinear optical characteristics of PVA/PVP polymeric blend using Co0.9Cu0.1S nanoparticles for optical and photonic applications. Opt. Mater. **127**, 112255 (2022)

Alhazime, A.A., Barakat, M.M., Benthami, K., Nouh, S.A.: Gamma irradiation-induced modifications in the structural, thermal, and optical properties of polyvinyl alcohol-polyethylene glycol/cobalt oxide nanocomposite films. J. Vinyl Additive Technol. **27**(2), 347–355 (2021)

Alhazime, A.A., Benthami, K.A., Alsobhi, B.O., Ali, G.W., Nouh, S.A.: Pani-Ag/PVA nanocomposite: gamma induced changes in the thermal and optical characteristics. J. Vinyl Add. Tech. **27**(1), 47–53 (2021)

Alosabi, A.Q., Al-Muntaser, A.A., El-Nahass, M.M., Oraby, A.H.: Effect of heat treatment on structure, surface morphology, linear and nonlinear optical properties of Na2Pc films for optoelectronic applications. Opt. Laser Technol. **158**, 108846 (2023)

Alshahrani, B., ElSaeedy, H.I., Fares, S., Korna, A.H., Yakout, H.A., Maksoud, M.I.A.A., Fahim, R.A., Ashour, A.H., Awed, A.S.: The effect of gamma irradiation on structural, optical, and dispersion

properties of PVA/Zn0.5Co0.4Ag0$_2$Fe$_2$O$_4$ nanocomposite films. J. Mater. Sci. Mater. Electron. **32**(10), 13336–13349 (2021a)

Alshahrani, B., ElSaeedy, H.I., Korna, A.H., Yakout, H.A., Ashour, A.H., Maksoud, M.A., Fahim, R.A., Awed, A.S.: Revealing the effect of gamma irradiation on structural, ferromagnetic resonance, optical, and dispersion properties of PVC/Mn0.5Zn0.5Fe$_2$O$_4$ nanocomposite films. Opt. Mater. **1**(118), 111216 (2021b)

Aly, K.: Adjusting the relation between the imaginary part of the dielectric constant and the wavelength. Physica B **655**, 414723 (2023)

Azad, H., Mohsennia, M.: A novel free-standing polyvinyl butyral-polyacrylonitrile/ZnAl-layered double hydroxide nanocomposite membrane for enhanced heavy metal removal from wastewater. J. Membr. Sci. **615**, 118487 (2020)

Badawi, A., Alharthi, S.S., Mostafa, N.Y., Althobaiti, M.G., Altalhi, T.: Effect of carbon quantum dots on the optical and electrical properties of polyvinylidene fluoride polymer for optoelectronic applications. Appl. Phys. A **125**(12), 858 (2019)

Badawi, A., Alsufyani, S.J., Alharthi, S.S., Althobaiti, M.G., Alkathiri, A.A., Almurayshid, M., Alharbi, A.N.: Impact of gamma irradiation on the structural, linear and nonlinear optical properties of lead oxide incorporated PVA/graphene blend for shielding applications. Opt. Mater. **127**, 112244 (2022)

Batool, M., Nazar, M.F., Awan, A., Tahir, M.B., Rahdar, A., Shalan, A.E., Lanceros-Méndez, S., Zafar, M.N.: Bismuth-based heterojunction nanocomposites for photocatalysis and heavy metal detection applications. Nano-Struct. Nano-Objects **27**, 100762 (2021)

Beecroft, L.L., Ober, C.K.: Nanocomposite materials for optical applications. Chem. Mater. **9**(6), 1302–1317 (1997)

Beena, P., Jayanna, H.: Dielectric studies and AC conductivity of piezoelectric barium titanate ceramic polymer composites. Polym. Polym. Compos. **27**(9), 619–625 (2019)

Bekhit, M., Abo El Naga, A.O., El Saied, M., Abdel Maksoud, M.I.A.: Radiation-induced synthesis of copper sulfide nanotubes with improved catalytic and antibacterial activities. Environ. Sci. Pollut. Res. **28**(32), 44467–44478 (2021)

Bhat, N., Nate, M., Kurup, M., Bambole, V., Sabharwal, S.: Effect of γ-radiation on the structure and morphology of polyvinyl alcohol films. Nucl. Instrum. Methods Phys. Res., Sect. B **237**(3–4), 585–592 (2005)

Chen, Y., Liu, Y., Xie, X., Li, C., Si, Y., Zhang, M., Yan, Q.: Synthesis flower-like BiVO4/BiOI core/shell heterostructure photocatalyst for tetracycline degradation under visible-light irradiation. J. Mater. Sci. Mater. Electron. **30**(10), 9311–9321 (2019)

Choudhary, S.: Structural, optical, dielectric and electrical properties of (PEO–PVP)–ZnO nanocomposites. J. Phys. Chem. Solids **121**, 196–209 (2018)

Dabodiya, T.S., Selvarasu, P., Murugan, A.V.: Tetragonal to monoclinic crystalline phases change of BiVO4 via microwave-hydrothermal reaction: in correlation with visible-light-driven photocatalytic performance. Inorg. Chem. **58**(8), 5096–5110 (2019)

Devi, C.U., Sharma, A., Rao, V.N.: Electrical and optical properties of pure and silver nitrate-doped polyvinyl alcohol films. Mater. Lett. **56**(3), 167–174 (2002)

Dhatarwal, P., Sengwa, R.J.: Nanofiller controllable optical parameters and improved thermal properties of (PVP/PEO)/Al2O3 and (PVP/PEO)/SiO$_2$ nanocomposites. Optik **233**, 166594 (2021)

Dhatarwal, P., Sengwa, R.J., Choudhary, S.: Multifunctional (PVP/PEO)/SnO$_2$ nanocomposites of tunable optical and dielectric properties. Optik **221**, 165368 (2020)

E.D. Palik, Handbook of Optical Constants of Solids (Academic, Orlando, 1985), Google Scholar 286–297.

Ebnalwaled, A.A., Thabet, A.: Controlling the optical constants of PVC nanocomposite films for optoelectronic applications. Synth. Met. **220**, 374–383 (2016)

Eisa, W.H., Abdel-Moneam, Y.K., Shaaban, Y., Abdel-Fattah, A.A., Abou Zeid, A.M.: Gamma-irradiation assisted seeded growth of Ag nanoparticles within PVA matrix. Mater. Chem. Phys. **128**(1–2), 109–113 (2011)

El- Mallah, H.M., Abd- El Salam, M., El- Damhogi, D.G., Elesh, E.: Structural characterization and optical parameter of silicon phthalocyanine dichloride thin films dependence with gamma ray radiation. Radiat. Phys. Chem. **176**, 109012 (2020)

El-Bana, M.S., Fouad, S.S.: Opto-electrical characterisation of As33Se67−xSnx thin films. J. Alloy. Compd. **695**, 1532–1538 (2017)

El-Ghamaz, N., El-Sonbati, A., El-Mogazy, M.: Effect of γ-radiation on the structural and optical properties of poly (3-allyl-5-[(4-nitrophenyl) diazenyl]-2-thioxothiazolidine-4-one) thin films. J. Mol. Liq. **248**, 556–563 (2017)

El-Malawy, D., Al-Abyad, M., El Ghazaly, M., Abdel Samad, S., Hassan, H.E.: γ-ray effects on PMMA polymeric sheets doped with CdO nano particles. Radiat. Phys. Chem. **184**, 109463 (2021)

Emara, A.M., Makhlouf, M., Yousef, E.S.: Influence of temperature-induced nanocrystallization on the optical properties of Ni+ 2-containing glassy tellurite thin films. J. Non-Cryst. Solids **515**, 58–67 (2019)
Fink, D., Chung, W., Klett, R., Schmoldt, A., Cardoso, J., Montiel, R., Vazquez, M., Wang, L., Hosoi, F., Omichi, H.: Carbonaceous clusters in irradiated polymers as revealed by UV-Vis spectrometry. Radiat. Eff. Defects Solids **133**(3), 193–208 (1995)
Frumar, M., Jedelský, J., Frumarova, B., Wagner, T., Hrdlička, M.: Optically and thermally induced changes of structure, linear and non-linear optical properties of chalcogenides thin films. J. Non-Cryst. Solids **326**, 399–404 (2003)
García-Pérez, U., Sepúlveda-Guzmán, S., Martinez-de La Cruz, A., Peral, J.: Selective synthesis of monoclinic bismuth vanadate powders by surfactant-assisted co-precipitation method: Study of their electrochemical and photocatalytic properties. Int. J. Electrochem. Sci **7**, 9622–9632 (2012)
Guo, M., He, Q., Wang, A., Wang, W., Fu, Z.: A novel, simple and green way to fabricate $BiVO_4$ with excellent photocatalytic activity and its methylene blue decomposition mechanism. Crystals **6**(7), 81 (2016)
Hajian, M., Reisi, M.R., Koohmareh, G.A., Zanjani Jam, A.R.: Preparation and characterization of polyvinylbutyral/graphene nanocomposite. J. Polym. Res. **19**, 1–7 (2012)
Holzwarth, U., Gibson, N.: The Scherrer equation versus the "Debye–Scherrer equation." Nat. Nanotechnol. **6**(9), 534–534 (2011)
Ipakchi, H., Rezadoust, A.M., Esfandeh, M., Rezaei, M.: An investigation on the effect of polyvinyl butyral interlayer forms on the fracture toughness of glass reinforced phenolic laminates. Thin-Walled Struct. **151**, 106724 (2020)
Kassem, S.M., Abdel Maksoud, M.I., El Sayed, A.M., Ebraheem, S., Helal, A.I., Ebaid, Y.Y.: Optical and radiation shielding properties of PVC/$BiVO_4$ nanocomposite. Sci. Rep. **13**(1), 10964 (2023)
Khan, I., Ali, S., Mansha, M., Qurashi, A.: Sonochemical assisted hydrothermal synthesis of pseudo-flower shaped Bismuth vanadate (BiVO4) and their solar-driven water splitting application. Ultrason. Sonochem. **36**, 386–392 (2017)
Krumhansl, J.: The solid state. Annu. Rev. Phys. Chem. **8**(1), 77–104 (1957)
Lee, K.-S., Lu, T.-M., Zhang, X.-C.: The measurement of the dielectric and optical properties of nano thin films by THz differential time-domain spectroscopy. Microelectron. J. **34**(1), 63–69 (2003)
Lee, D.J., Yoon, I.S., Park, C.H., Choi, J., Park, Y.W., Ju, B.-K.: Extraction of light using random nanocone on poly(vinyl-butyral) for flexible OLEDs. Sci. Rep. **9**(1), 12312 (2019)
Lei, Z., Chen, Z., Peng, H., Shen, Y., Feng, W., Liu, Y., Zhang, Z., Chen, Y.: Fabrication of highly electrical conductive composite filaments for 3D-printing circuits. J. Mater. Sci. **53**(20), 14495–14505 (2018)
Lei, Z., Chen, Z., Zhou, Y., Liu, Y., Xu, J., Wang, D., Shen, Y., Feng, W., Zhang, Z., Chen, H.: Novel electrically conductive composite filaments based on Ag/saturated polyester/polyvinyl butyral for 3D-printing circuits. Compos. Sci. Technol. **180**, 44–50 (2019)
Li, X., Wang, C., Ma, L., Liu, L.: Ellipsometry-transmission measurement of the complex refractive indices for a series of organic solvents in the 200–1700 nm spectral range. Infrared Phys. Technol. **125**, 104313 (2022)
Maksoud, M.A., Bekhit, M., El-Sherif, D.M., Sofy, A.R., Sofy, M.R.: Gamma radiation-induced synthesis of a novel chitosan/silver/Mn-Mg ferrite nanocomposite and its impact on cadmium accumulation and translocation in brassica plant growth. Int. J. Biol. Macromol. **1**(194), 306–316 (2022)
Maksoud, M.I.A.A., Kassem, S.M., Bekhit, M., Fahim, R.A., Ashour, A.H., Awed, A.S.: Gamma radiation shielding properties of poly(vinyl butyral)/Bi2O3@BaZrO3 nanocomposites. Mater. Chem. Phys. **268**, 124728 (2021)
Mohammadian-Kohol, M., Asgari, M., Shakur, H.R.: A detailed investigation of the gamma-ray radiation effects on the optical properties of polyvinyl butyral film. Optik **127**(19), 7459–7468 (2016)
Morad, I., Alshehri, A.M., Mansour, A.F., Wasfy, M.H., El-Desoky, M.M.: Facile synthesis and comparative study for the optical performance of different TiO_2 phases doped PVA nanocomposite films. Physica B **597**, 412415 (2020)
Nguyen, T.-P.: Polymer-based nanocomposites for organic optoelectronic devices. Rev. Surf. Coat. Technol. **206**(4), 742–752 (2011)
Nouh, S.A., Benthami, K.: Gamma induced changes in the structure and optical properties of ZnS/PVA nanocomposite. J. Vinyl Add. Tech. **25**(3), 271–277 (2019)
Nouh, S., Benthami, K., Massoud, A., El-Shamy, N.: Effect of gamma irradiation on the structural and optical properties of PVA/CdS nanocomposite films prepared by ex-situ technique. Radiat. Eff. Defects Solids **173**(11–12), 956–969 (2018)
Pookmanee, P., Kojinok, S., Phanichphant, S.: Photocatalytic degradation of 2, 4-dichlorophenol using BiVO4 powder prepared by the sol–gel method. Trans. Mater. Res. Soc. Jpn **39**(4), 431–434 (2014)
Pookmanee, P., Kojinok, S., Puntharod, R., Sangsrichan, S., Phanichphant, S.: Preparation and characterization of BiVO4 powder by the sol-gel method. Ferroelectrics **456**(1), 45–54 (2013)

Reheem, A.A., Maksoud, M.A., Ashour, A.: Surface modification and metallization of polycarbonate using low energy ion beam. Radiat. Phys. Chem. **125**, 171–175 (2016)
Reyes-Coronado, A., Ortíz-Solano, C.G., Zabala, N., Rivacoba, A., Esquivel-Sirvent, R.: Analysis of electromagnetic forces and causality in electron microscopy. Ultramicroscopy **192**, 80–84 (2018)
Saadeddin, I., Pecquenard, B., Manaud, J.-P., Decourt, R., Labrugère, C., Buffeteau, T., Campet, G.: Synthesis and characterization of single-and co-doped SnO_2 thin films for optoelectronic applications. Appl. Surf. Sci. **253**(12), 5240–5249 (2007)
Sahoo, D., Naik, R.: A review on the linear/nonlinear optical properties of Se doped chalcogenide thin films as potential optoelectronic applications. J. Non-Cryst. Solids **597**, 121934 (2022)
Sell, D., Casey, H., Jr., Wecht, K.: Concentration dependence of the refractive index for *n*-and *p*-type GaAs between 1.2 and 1.8 eV. J. Appl. Phys. **45**(6), 2650–2657 (1974)
Shao, P.-W., Lin, M.-C., Zhuang, Q., Huang, J., Liu, S., Chen, H.-W., Liu, H.-L., Lu, Y.-J., Hsu, Y.-J., Wu, J.-M., Chen, Y.-C., Chu, Y.-H.: Flexo-phototronic effect in centro-symmetric $BiVO_4$ epitaxial films. Appl. Catal. B **312**, 121367 (2022)
Siva, V., Vanitha, D., Murugan, A., Shameem, A., Bahadur, S.A.: Studies on structural and dielectric behaviour of PVA/PVP/SnO nanocomposites. Compos. Commun. **23**, 100597 (2021)
Soliman, T., Vshivkov, S.: Effect of Fe nanoparticles on the structure and optical properties of polyvinyl alcohol nanocomposite films. J. Non-Cryst. Solids **519**, 119452 (2019)
Stepanov, A.L.: Optical properties of polymer nanocomposites with functionalized nanoparticles, pp. 325–355. Elsevier, Polymer Composites with Functionalized Nanoparticles (2019)
Taha, T.A.: Optical properties of PVC/Al2O3 nanocomposite films. Polym. Bull. **76**(2), 903–918 (2019)
Taha, T.A., Alzara, M.A.A.: Synthesis, thermal and dielectric performance of PVA-$SrTiO_3$ polymer nanocomposites. J. Mol. Struct. **1238**, 130401 (2021)
Tian, T., Fang, Y., Wang, W., Yang, M., Tan, Y., Xu, C., Zhang, S., Chen, Y., Xu, M., Cai, B., Wu, W.-Q.: Durable organic nonlinear optical membranes for thermotolerant lightings and in vivo bioimaging. Nat. Commun. **14**(1), 4429 (2023)
Ticha, H., Tichy, L.: Semiempirical relation between non-linear susceptibility (refractive index), linear refractive index and optical gap and its application to amorphous chalcogenides. J. Optoelectron. Adv. Mater **4**(2), 381–386 (2002a)
Ticha, H., Tichy, L.: Semiempirical relation between non-linear susceptibility (refractive index), linear refractive index and optical gap and its application to amorphous chalcogenides. J. Optoelectron. Adv. Mater. **4**(2), 381–386 (2002b)
Urbach, F.: The long-wavelength edge of photographic sensitivity and of the electronic absorption of solids. Phys. Rev. **92**(5), 1324 (1953)
Waszkowska, K., Krupka, O., Kharchenko, O., Figà, V., Smokal, V., Kutsevol, N., Sahraoui, B.: Influence of ZnO nanoparticles on nonlinear optical properties. Appl. Nanosci. **10**, 4977–4982 (2020)
Wemple, S., DiDomenico, M., Jr.: Behavior of the electronic dielectric constant in covalent and ionic materials. Phys. Rev. B **3**(4), 1338 (1971)
Wen, B., Wang, X., Zhang, Y.: Ultrathin and anisotropic polyvinyl butyral/Ni-graphite/short-cut carbon fibre film with high electromagnetic shielding performance. Compos. Sci. Technol. **169**, 127–134 (2019)
Zeyada, H., El-Nahass, M., Elashmawi, I., Habashi, A.: Annealing temperatures induced optical constant variations of methyl violet 2B thin films manufactured by the spin coating technique. J. Non-Cryst. Solids **358**(3), 625–636 (2012)
Zidan, H.: Electron spin resonance and ultraviolet spectral analysis of UV-irradiated PVA films filled with $MnCl_2$ and CrF_3. J. Appl. Polym. Sci. **88**(1), 104–111 (2003)